Mixed Transition Metal-Gold Cluster Hydrides

Bruce D. Alexander, Brian J. Johnson, Steven M. Johnson, Albert L. Casalnuovo, and L. H. Pignolet*

Contribution from the Department of Chemistry, University of Minnesota, Minneapolis, Minnesota 55455. *Received December 27, 1985*

Abstract: Four new transition metal-gold hydride compounds have been synthesized. $[Au_2Ru(H)_2(dppm)_2(PPh_3)_2](NO_3)_2$ (**1**), $[AuIr(H)_2(bipy)(PPh_3)_3](BF_4)_2$ (**2**), and $[AuIrH(CO)(PPh_3)_4]PF_6$ (**4**) were made by the reaction of $AuPPh_3NO_3$ with $Ru(H)_2(dppm)_2$, $[Ir(H)_2(bipy)(PPh_3)_2]BF_4$, and $IrH(CO)(PPh_3)_3$, respectively, and $[AuIrH(PPh_3)_4]X$ (X = BF_4, NO_3 mixture) (**5**) was made by the reaction of PPh_3 with $[Au_2IrH(NO_3)(PPh_3)_4]BF_4$. Compounds **1** and **2** were characterized by single-crystal X-ray diffraction in the solid state [**1**, $P\bar{1}$, a = 15.022 (4) Å, b = 19.247 (5) Å, c = 14.783 (5) Å, α = 104.64 (2)°, β = 113.68 (2)°, γ = 87.05 (2)°, T = -50 °C R = 0.026; **2**, $P2_12_12_1$, a = 11.908 (5) Å, b = 20.876 (3) Å, c = 20.061 (3) Å, $\alpha = \beta = \gamma$ = 90°, T = -50 °C, R = 0.041] and by ^{31}P and ^1H NMR spectroscopies in solution. In **1** the hydride ligands were directly observed by X-ray diffraction and are bridging the Ru to Au bonds. The average Ru-H and Au-H distances are 1.61 (4) and 1.77 (4) Å, respectively, and the average Ru-Au and Au-Au separations are 2.781 (0) and 2.933 (0) Å, respectively. In **2** the hydride ligands were not directly located but are thought to be dibridging the Ir to Au bond (2.699 (0) Å). In both compounds the bridging hydride formulations were confirmed by NMR and IR spectroscopies. In compounds **4** and **5** the hydride ligands are not interacting with Au but are terminally bonded to the Ir. In these latter compounds the Ir-H stretch was easily observed by IR spectroscopy [**4**, 2060 cm^{-1}; **5**, 2080 cm^{-1}], while no absorptions in the terminal hydride region were observed for **1** and **2**. The bridging hydride region in the IR was obscured by other ligand absorptions, so bridging hydride vibrations were not observed.

Gold-hydride interactions are rare although they are likely in gold surface catalyzed H_2/D_2 exchange and olefin hydrogenation reactions[1] and in the reduction of $AuPPh_3NO_3$ by H_2 in EtOH solution to give gold phosphine clusters.[2] Monometallic gold hydride compounds have not been directly observed, but several heterobimetallic complexes are known in which a hydride ligand bridges between a transition metal and a gold atom.[3,4] In one of these compounds, $AuCr(\mu\text{-}H)(CO)_5(PPh_3)$, the bridging hydride was directly observed by X-ray diffraction,[3] while in the other, $[AuIr(\mu\text{-}H)(H)_2(PPh_3)_4]BF_4$, its bridging position was deduced by X-ray diffraction and ^{31}P and ^1H NMR spectroscopies.[4] A variety of transition metal-gold hydride clusters have recently been prepared in our laboratory.[5-8] For example, $[Au_5Re(H)_4(PPh_3)_7](PF_6)_2$,[5] $[Au_3RhH(CO)(PPh_3)_5]PF_6$,[5] $[Au_4Ir(H)_2(PPh_3)_6]BF_4$,[6] $[Au_2IrH(PPh_3)_4(NO_3)]BF_4$,[7] and $[AuIr_3(H)_6(dppe)_3(NO_3)]BF_4$[8] (dppe = bis[1,2-(diphenylphosphino)ethane]) were characterized by single-crystal X-ray diffraction. The hydride ligands in these clusters were not located, although M(μ-H)Au bonding was considered likely in most based on structural, NMR, and IR data.[5-8]

In this paper we report the synthesis, single-crystal X-ray analysis, and spectroscopic characterization of two new transition metal-gold hydride clusters, $[Au_2Ru(H)_2(dppm)_2(PPh_3)_2](NO_3)_2$ (**1**) and $[AuIr(H)_2(bipy)(PPh_3)_3](BF_4)_2$ (**2**). In **1** the hydride ligands were located and refined in the X-ray analysis and were found to be bridging between the Au and Ru atoms. In **2** the hydrides were not located in the X-ray analysis, but the structural and spectroscopic data strongly support a bridging mode. The results of this study lend support to a bridging hydride assignment in many of these gold alloy clusters (vide infra). The structures and reactivity of these transition metal-gold hydride clusters are important in understanding gold and gold alloy surface catalysis.[1,9] For this reason it is especially important to fully elucidate the bonding modes of the hydride ligands in these and related compounds. The synthesis and spectroscopic characterization of several other new Ir-Au hydride compounds are also reported in this paper.

Experimental Section

Physical Measurements and Reagents. ^1H and ^{31}P NMR spectra were recorded at 300 and 121.5 MHz, respectively, with the use of a Nicolet NT-300 spectrometer. ^{31}P chemical shifts are reported in parts per million (ppm) relative to the internal standard trimethyl phosphate. Infrared spectra were recorded on a Beckman Model 4250 grating spectrometer. Conductivity measurements were made with the use of a Yellow Springs Model 31 conductivity bridge. Compound concentrations used in the conductivity experiments were between 10^{-3} and 10^{-4} with use of CH_3CN as the solvent. Microanalyses were carried out by M-H-W laboratories, Phoenix, AZ. Solvents were dried and distilled prior to use. $AuPPh_3NO_3$,[10] $[Au_2IrH(PPh_3)_4NO_3]BF_4$,[7,11] $[Ir(H)_2(PPh_3)_2(acetone)_2]BF_4$,[12] $IrH(CO)(PPh_3)_3$,[13] and $Ru(H)_2(dppm)_2$[14] were prepared as described in the literature. Bis(diphenylphosphino)methane, dppm, was purchased from Strem Chemicals, Inc., and 2,2'-bipyridine, bipy, was purchased from Eastman Organic Chemicals. All manipulations were carried out under a purified N_2 atmosphere with use of standard Schlenk techniques unless otherwise noted.

Preparation of Compounds. $[Au_2Ru(H)_2(dppm)_2(PPh_3)_2](NO_3)_2$, **1**, was prepared by the reaction of $Ru(H)_2(dppm)_2$ (98 mg, 0.11 mmol) with $AuPPh_3NO_3$ (108 mg, 0.21 mmol) with the use of 5 mL of acetone as solvent. The resulting light-yellow solution was stirred at ambient temperature for 1 h. An off-white powder began to precipitate from this solution during stirring and complete precipitation occurred upon the addition of 10 mL of Et_2O. The solid was filtered and washed with Et_2O, and upon recrystallization from CH_2Cl_2-Et_2O, dark-yellow rectangular crystals of **1** were isolated in 65% yield. $^{31}P\{^1H\}$ NMR (CH_2Cl_2, 25 °C): δ 41.2 (pseudo d of q, J = 36.2 and 8.5 Hz, int = 1), -1.82 (t of t, J = 33.2 and 8.5 Hz, int = 1), -8.05 (mult, int = 1). ^1H NMR in hydride

(1) Schwank, J. *Gold Bull.* **1983**, *16*, 103.
(2) Bos, W.; Bour, J. J.; Steggerda, J. J.; Pignolet, L. H. *Inorg. Chem.*, in press.
(3) Green, M.; Orpen, A. G.; Salter, I. D.; Stone, F. G. A. *J. Chem. Soc., Dalton Trans.* **1984**, 2497.
(4) Lehner, H.; Matt, D.; Pregosin, P. S.; Venanzi, L. M. *J. Am. Chem. Soc.* **1982**, *104*, 6825.
(5) Boyle, P. D.; Johnson, B. J.; Buehler, A.; Pignolet, L. H. *Inorg. Chem.* **1986**, *25*, 5.
(6) Casalnuovo, A. L.; Casalnuovo, J. A.; Nilsson, P. V.; Pignolet, L. H. *Inorg. Chem.* **1985**, *24*, 2554.
(7) Casalnuovo, A. L.; Laska, T.; Nilsson, P. V.; Olofson, J.; Pignolet, L. H.; Bos, W.; Bour, J. J.; Steggerda, J. J. *Inorg. Chem.* **1985**, *24*, 182.
(8) Casalnuovo, A. L.; Pignolet, L. H.; van der Velden, J. W. A.; Bour, J. J.; Steggerda, J. J. *J. Am. Chem. Soc.* **1983**, *105*, 5957.
(9) Sinfelt, J. H. *Bimetallic Catalysis*; Wiley: New York, 1983; Chapter 2. Wachs, I. E. *Gold Bull.* **1983**, *16*, 98.
(10) Malatesta, J.; Naldini, L.; Simonetta, G.; Cariati, F. *Coord. Chem. Rev.* **1966**, *1*, 255.
(11) Casalnuovo, A. L. Ph.D. Thesis, University of Minnesota, 1984.
(12) Shapley, J. R.; Schrock, R. R.; Osborn, J. A. *J. Am. Chem. Soc.* **1969**, *91*, 2816.
(13) Wilkinson, G. *Inorg. Synth.* **1971**, *13*, 126.
(14) Chaudret, B.; Commenges, G.; Poilblanc, R. *J. Chem. Soc., Dalton Trans.* **1984**, 1635.

0002-7863/86/1508-4409$01.50/0

Table I. Summary of Crystal Data and Intensity Collection for **1** and **2**

cryst parameters/measment of intensity data	$[Au_2Ru(H)_2(dppm)_2(PPh_3)_2](NO_3)_2$, **1**	$[AuIr(H)_2(bipy)(PPh_3)_3](BF_4)_2 \cdot CH_2Cl_2 \cdot (C_2H_5)_2O$, **2**
cryst system	triclinic	orthorhombic
space group	$P\bar{1}$ (No. 2)	$P2_12_12_1$ (No. 19)
cryst dimensions, mm^3	0.4 × 0.4 × 0.5	0.35 × 0.25 × 0.10
cell parameters at T, °C	−50	−50
a, Å	15.022 (4)	11.908 (5)
b, Å	19.247 (5)	20.876 (3)
c, Å	14.783 (5)	27.061 (3)
α, deg	104.64 (2)	90
β, deg	113.68 (2)	90
γ, deg	87.05 (2)	90
V, $Å^3$	3781 (4)	6728 (5)
Z	2	4
calcd density, g cm^{-3}	1.681	1.643
abs. coeff, cm^{-3}	42.37	43.56
max, min, av transmission factors	1.00, 0.83, 0.90	1.00, 0.92, 0.96
formula	$C_{86}H_{76}N_2O_6P_6Au_2Ru$	$C_{69}H_{65}B_2Cl_2F_8N_2OP_3AuIr$
fw, amu	1914.42	1664.79
diffractometer	CAD 4	
radiation	Mo Kα (λ = 0.71069 Å) graphite monochromatized	
scan type range, 2θ, deg	ω, 6–48	ω, 6–54
unique reflections measd (region)	11852 (+h,±k,±l)	8038 (+h,+k,+l)
obsd reflections[a]	9904[$F_{o2} \geq 3\sigma(F_o^2)$]	5713[$F_o^2 \geq 3\sigma(F_o^2)$]
refinement by full-matrix least squares		
no. of parameters	935	423
R[b]	0.026	0.041
R_w[b]	0.033	0.045
GOF[b]	1.55	1.52
p[a]	0.03	0.03

[a] The intensity data were processed as described in: *CAD 4 and SDP-PLUS User's Manual*; B. A. Frenz & Assoc.: College Station, TX, 1982. The net intensity $I = [K(NPI)](C - 2B)$, where K = 20.1166 (attenuator factor), NPI = ratio of fastest possible scan rate to scan rate for the measurement, C = total count, and B = total background count. The standard deviation in the net intensity is given by $[\sigma(I)]^2 = (K/NPI)^2[C + 4B + (pI)^2]$ where p is a factor used to downweight intense reflections. The observed structure factor amplitude F_o is given by $F_o = (I/Lp)^{1/2}$, where Lp = Lorentz and polarization factors. The $\sigma(I)$'s were converted to the estimated errors in the relative structure fators $\sigma(F_o)$ by $\sigma(F_o) = {}^1/_2[\sigma(I)/I]F_o$. [b] The function minimized was $\sum w(|F_o| - |F_c|)^2$, where $w = 1/[\sigma(F_o)]^2$. The unweighted and weighted residuals are defined as $R = (||F_o| - |F_c||)/\sum|F_o|$ ands $R_w = [(\sum w(|F_o| - |F_c|))^2/(\sum w|F_o|)^2]^{1/2}$. The error is an observation of unit weight (GOF) is $[\sum w(|F_o| - |F_c|)^2/(NO - NV)]^{1/2}$, where NO and NV are the number of observations and variables, respectively.

region (CD_2Cl_2, 25 °C): δ −4.62 (pseudo d of q, J = 74.8 and ca. 7 Hz). The NMR spectra are described in detail in the text and are shown in Figures 3 and 4. IR peaks were not observed in the 1800–2300-cm^{-1} region. Equivalent conductance (148 Ω^{-1} cm^2 $equiv^{-1}$) is indicative of a 1:2 electrolyte in CH_3CN solution. Anal. Calcd for $Au_2RuP_6C_{86}H_{76}N_2O_6$: C, 53.96; H, 4.00; N, 1.46. Found: C, 54.18; H, 4.16; N, 1.51.

$[Ir(H)_2(bipy)(PPh_3)_2]BF_4$ was prepared from $[Ir(H)_2(PPh_3)_2(acetone)_2]BF_4$[12] by the addition of a 3-fold molar excess of bipyridine in acetone solution.[15] Upon reduction of the volume of the yellow solution, some crystals began to form. At this point the addition of Et_2O resulted in the precipitation of yellow microcrystals in 74% yield. The compound was determined to be pure by NMR. $^{31}P\{^1H\}$ NMR (CH_2Cl_2, 25 °C): δ 17.98 (s). ^1H NMR (acetone-d_6, 25 °C): δ −19.4 (t, J = 17 Hz). IR (KBr disk) in terminal hydride region: 2140, 2215 cm^{-1}. The NMR and IR data were similar but distinctly different from those of the parent compound $[Ir(H_2)(PPh_3)_2(acetone)_2]BF_4$.[12]

$[AuIr(H)_2(bipy)(PPh_3)_3](BF_4)_2$, 2, was prepared by reaction of an acetone solution of $[Ir(H)_2(bipy)(PPh_3)_2]BF_4$ (10 mL, 156 mg, 0.16 mmol) with an acetone solution of $AuPPh_3NO_3$ (10 mL, 169 mg, 0.32 mmol) at −60 °C. The color of the solution immediately changed from yellow to colorless. The solution was stirred for an hour and was slowly warmed to room temperature. A white precipitate formed during this process. Et_2O (20 mL) was added, and the precipitate was collected by filtration. The white solid was washed with Et_2O, dried in vacuo, and then dissolved in a minimal amount of MeOH. The MeOH solution was filtered into a flask which contained 273 mg of $NaBF_4$, and an off-white precipitate formed during stirring. The solid was collected and recrystallized from a CH_2Cl_2–Et_2O solvent mixture, giving 182 mg of white microcrystalline **2** (75% yield). Large crystals of **2** as a CH_2Cl_2–Et_2O solvate were obtained by slow solvent diffusion of Et_2O into a CH_2Cl_2 solution of **2**. These crystals readily lost solvent and became opaque when removed from the crystallizing solution. $^{31}P\{^1H\}$ NMR (CH_2Cl_2, 25 °C): δ 46.5 (s, int = 1), 2.98 (s, int = 2). ^1H NMR in hydride region ($CDCl_3$, 25 °C): δ −13.3 (d of t, J = 31 and 11 Hz). IR peaks were not observed in the 1800–2300-cm^{-1} region. Equivalent conductance (200 Ω^{-1} cm^2 $equiv^{-1}$) is indicitive of a 1:2 electrolyte in CH_3CN solution. Anal. Calcd for $AuIrP_3C_{64}H_{55}N_2B_2F_8$: C, 50.98; H, 3.68; N, 1.86; P, 6.16. Found: C, 51.16; H, 3.90; N, 1.89; P, 6.09.

$[AuIrH(CO)(PPh_3)_4]PF_6$, 4, was prepared by the reaction of $IrH(CO)(PPh_3)_3$ (350 mg, 348 mmol) with $AuPPh_3NO_3$ (181 mg, 348 mmol) in toluene at −78 °C. The resulting suspension was stirred and slowly warmed to room temperature during a 3-h period. An orange-yellow precipitate remained which was filtered and washed with toluene and Et_2O and dried in vacuo. The solid was then dissolved in MeOH and filtered into a MeOH solution which contained 300 mg of KPF_6. At tan microcrystalline precipitate formed and was filtered, washed with cold MeOH and Et_2O, and dried in vacuo. The yield was 376 mg (67%). $^{31}P\{^1H\}$ NMR (CH_2Cl_2, −40 °C): δ 37.5 (d, J = 99 Hz, int = 1), 7.37 (d, J = 99 Hz, int = 1), 4.8 (s, int = 2). The molecule is nonrigid (see Discussion in text). ^1H NMR (acetone-d_6, 25 °C): δ −8.9 (q, J_{PH} = 17 Hz). IR (KBr disk) in 1800–2300-cm^{-1} region: ν_{CO} 1956 (s), ν_{IrH} 2060 (m) cm^{-1}. Equivalent conductance (88.6 Ω^{-1} cm^2 $equiv^{-1}$) is indicative of a 1:1 electrolyte in CH_3CN solution. Anal. Calcd for $AuIrP_5C_{73}H_{61}O_1F_6$: C, 54.38; H, 3.81; P, 9.60. Found: C, 54.60; H, 4.06; P, 9.46.

$[AuIrH(PPh_3)_4]X$ (X = BF_4, NO_3 mixture), 5, was prepared by the reaction at −5 °C of $[Au_2IrH(NO_3)(PPh_3)_4]BF_4$ (100 mg, 0.056 mmol) suspended in 3 mL of EtOH with PPh_3 (30 mg, 0.11 mmol) dissolved in a minimal amount of Et_2O. During the reaction the solid dissolved, giving an orange solution. This solution was stirred at about −20 °C for 1 h and a yellow–orange solid precipitated upon the addition of cold Et_2O. The product was filtered at −20 °C and washed with cold Et_2O, giving a 50% isolated yield. The byproduct in this reaction was $[Au(PPh_3)_2]^+$ [$^{31}P\{^1H\}$ δ 41 (s)]. The reaction was quantitative in solution as evidenced by ^{31}P and ^1H NMR. $^{31}P\{^1H\}$ NMR (acetone, 0 °C): δ 28.1 (pseudo t, J = 9 Hz, int = 2), 19.5 (pseudo q, J = 10 Hz, int = 1), −6.6 (pseudo q, J = 8 Hz, int = 1). ^1H NMR (acetone-d_6, 0 °C) in the hydride region: δ −6.10 (d of t of d, J_{HP} = 99.5, 23.2, and 4.1 Hz). IR (KBr disk) in 1800–2300-cm^{-1} region: ν_{IrH} 2080 (w) cm^{-1}.

X-ray Structure Determination. Collection and Reduction of X-ray Data. A summary of crystal and intensity data for compounds **1** and **2** is presented in Table I. Crystals of both compounds were coated with a viscous high molecular weight hydrocarbon and secured to the end of glass fibers by cooling to −50 °C. The crystals remained stable at this

(15) Crabtree, R. H., private communication.

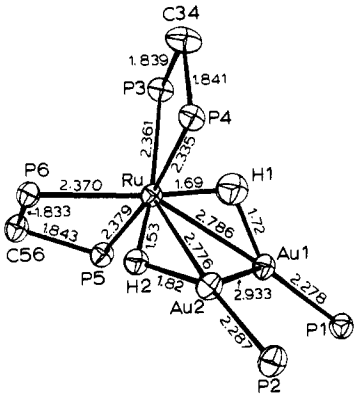

Figure 1. ORTEP drawing of the coordination core of **1** with selected distances. Ellipsoids are drawn with 50% probability boundaries. Phenyl rings have been omitted for clarity.

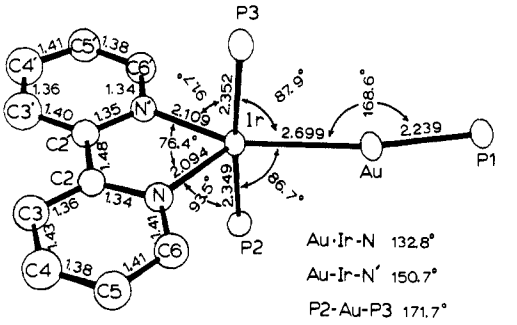

Figure 2. ORTEP drawing of the core of **2** with selected distances and angles. Ellipsoids are drawn with 50% probability boundaries. Phenyl rings have been omitted for clarity.

temperature during data collection. The crystal classes and space groups were unambiguously determined by the Enraf-Nonius CAD4-SDP-PLUS peak search, centering, and indexing programs,[16] by the presence or absence of systematic absences observed during data collection and by successful solution and refinement (vide infra). The intensities of three standard reflections were measured every 1.5 h of X-ray exposure time, and no decay was observed for either compound. Empirical absorption corrections were applied for both compounds by use of ψ-scan data and programs PSI and EAC.[16]

Solution and Refinement of the Structures. The structures were solved by conventional heavy atom techniques. The metal atoms were located by Patterson syntheses, and full-matrix least-squares refinement and difference Fourier calculations were used to locate all remaining non-hydrogen atoms. The atomic scattering factors were taken from the usual tabulation,[17] and the effects of anomalous dispersion were included in F_c by using Cromer and Ibers'[18] values of $\Delta f'$ and $\Delta f''$. Hdyrogen atom positions were calculated for all PPh_3, dppm, and bipy ligands and were included in the structure factor calculations but were not refined. All non-hydrogen atoms in **1** were refined with anisotropic thermal parameters except for N2 and O6 which were isotropic. One of the two NO_3^- anions was slightly disordered, but the distances and angles were reasonable. The two hydride ligands in **1** showed up clearly as the two highest peaks in a difference Fourier map based on the totally converged non-hydride-containing structure. These hydrides refined and converged with isotropic thermal parameters $B < 3$ Å^2 to give reasonable distances and angles (vide infra). The largest peaks in the final differences Fourier map of **1** were ca. 1 e Å^{-3} (approximate height of a hydrogen atom) and were located near the disordered N2 nitrate anion. In **2**, only the Au, IR, P, and F atoms were refined with anisotropic thermal parameters due to a shortage of observable data. Two solvate molecules (CH_2Cl_2 and Et_2O) per asymmetric unit were found in **2**. The final difference Fourier map did not reveal any peaks in the region where hydrides are possible. The largest peaks in this map were about 1 e Å^{-3} and were near the chlorine atoms of the CH_2Cl_2 solvate. Since the space group of **2** is acentric, a test for the correct chirality was performed. Both enantiomeric arrangements were tried, and the one reported gave a slightly better R factor (0.041 vs. 0.043).

The final positional and thermal parameters of the refined and calculated atoms are given in Tables II and III and as supplementary material.[19] ORTEP drawings of the dications including the labeling schemes are shown in Figures 1 and 2 and as supplementary material.[19]

Results and Discussion

$[Au_2Ru(H)_2(dppm)_2(PPh_3)_2](NO)_2$, 1. The addition of 2 equiv of $AuPPh_3NO_3$ to $Ru(H)_2(dppm)_2$ in acetone solution gave the dicationic gold-ruthenium dihydride cluster, **1**, in good yield. A single-crystal X-ray diffraction analysis of this compound was carried out in order to determine the nature of the ruthenium-gold interaction and the bonding mode of the two hydride ligands. These questions could not be answered from the solution NMR and IR data alone (vide infra).

The structure of the coordination core of the dication of **1** is shown in Figure 1, and distances and angles are given in Table IV. The structure consists of a cis bis-chelated $Ru(dppm)_2$ moiety bonded in a side-on fashion to a $Au_2(PPh_3)_2$ unit resulting in a tris-chelate-type stereochemistry around ruthenium. The hydrides are bridging between the Ru–Au bonds such that they are approximately trans to phosphorus atoms of the dppm chelates (H1–Ru–P6 169 (1)°; H2–Ru–P3 169 (1)°). The molecule possesses approximate C_2 symmetry with the C_2 axis bisecting the $RuAu_2$ triangle. The Au–P vectors are approximately trans to the Ru atom (P1–Au1–Ru 170.69 (3)°; P2–Au2–Ru 174.20 (3)°) and make angles of 147 (1)° and 155 (1)° with H1 and H2, respectively. H1 is symmetrically bridging within experimental error, and H2 bridges asymmetrically (1.53 (3) and 1.82 (3) Å for Ru–H2 and Au–H2, respectively). But this asymmetry is only slightly outside of experimental error and therefore not very significant. The average Ru–H and Au–H distances of 1.61 (4) and 1.77 (4) Å, respectively, are similar to values previously observed for hydrides bridging to Ru [1.62 (5) Å in $RuRh(\mu\text{-}H)(Ph)(cod)(PhPCH_2PPh_2)(dppm)$,[20] and typically range 1.6–1.9 Å[21]] and to Au [1.7 (1) Å in $AuCr(\mu\text{-}H)(CO)_5(PPh_3)^3$]. The Au–$\mu$-H distance is also reasonable in light of more precisely determined Os–H and Ir–μ-H distances.[21] The average Ru–H–Au angle of 111 (1)° is also similar to values observed in other M–H–M compounds[21] [111 (5)° in $AuCr(\mu\text{-}H)(CO)_5(PPh_3)^3$]. The Ru–Au distances are approximately equal (average 2.781 (0) Å) and are similar to values observed in other Ru–Au clusters [for example, average 2.837 (2) Å in $HRu_4Au_3(CO)_{12}(PPh_3)_3$[22] and 2.784 (2)–2.897 (2) Å in $Au_2Ru_3(\mu_3\text{-}S)(CO)_8(PPh_3)_3$[23]]. Although the Ru–Au distances in **1** are on the short end of the above range, it is not clear that this is a result of hydride bridge bonding. None of the known Ru–Au clusters have a simple $Ru(AuPPh_3)_2$ structure similar to **1**, so meaningful comparisons are not possible. The Au–Au separation of 2.933 (0) Å is within the range previously observed (2.73–3.22 Å) for such distances in heteronuclear metal clusters[5–8,23] and is only slightly longer than that (2.884 Å) in gold metal.[24] The Au–P distances (average 2.283 (1) Å) and Ru–P distances (average 2.361 (1) Å) are similar to values observed in other heterometallic clusters[5–8] and Ru(dppm)-chelated compounds,[20] respectively. There is not an obvious lengthening of the Ru–P bonds trans to the bridging hydrides

(16) All calculations were carried out on PDP 8A and 11/34 computers with the use of the Enraf-Nonius CAD 4-SDP-PLUS programs. This crystallographic computing package is described by: Frenz, B. A. In *Computing in Crystallography*; Schenk, H., Olthof-Hazekamp, R., van Konigsveld, H., Bassi, G. C., Eds.; Delft University: Delft, Holland, 1978; pp 64–71. Frenz, B. A. In *Structure Determination Package and SDP-PLUS User's Guide*; Frenz, B. A. & Assoc.: Inc., College Station, TX, 1982.

(17) Cromer, D. T.; Waber, J. T. *International Tables for X-Ray Crystallography*; Kynoch: Birmingham, England, 1974; Vol. IV, Table 2.2.4. Cromer, D. T. *Ibid.* Table 2.3.1.

(18) Cromer, D. T.,; Ibers, J. A. In ref 17.

(19) See paragraph at end of paper regarding supplementary material.

(20) Delavaux, B.; Chaudret, B.; Dahan, F.; Poilblanc, R. *Organometallics* **1985**, *4*, 935.

(21) Teller, R. G.; Bau, R. *Struct. Bonding (Berlin)* **1981**, *44*, 1; Bau, R.; Teller, R. G.; Kirtley, S. W.; Koetzle, T. F. *Acc. Chem. Res.* **1979**, *12*, 176.

(22) Bruce, M. I.; Nicholson, B. K. *J. Organomet. Chem.* **1983**, *252*, 243.

(23) Farrugia, L. J.; Freeman, M. J.; Green, M.; Orpen, A. G.; Stone, F. G. A.; Salter, I. D. *J. Organomet. Chem.* **1983**, *249*, 273.

(24) Pearson, W. B. *Lattice Spacings and Structures of Metals and Alloys*; Pergamon: London, 1951.

Table II. Table of Positional Parameters and Their Estimated Standard Deviations for **1**[a]

atom	X	Y	Z	B, Å²	atom	X	Y	Z	B, Å²
Au1	0.078 49 (1)	0.269 78 (1)	0.283 19 (1)	1.904 (3)	C3M	0.566 8 (4)	0.343 9 (3)	0.564 5 (3)	3.4 (1)
Au2	0.253 99 (1)	0.194 50 (1)	0.374 25 (1)	1.907 (3)	C3N	0.547 5 (4)	0.341 0 (4)	0.101 3 (4)	4.6 (1)
Ru	0.233 74 (2)	0.263 90 (2)	0.224 28 (2)	1.477 (7)	C4A	−0.167 3 (4)	0.503 9 (3)	0.250 8 (4)	3.5 (1)
H1	0.114 (3)	0.241 (2)	0.184 (3)	3 (1)*	C4B	0.013 7 (5)	0.328 1 (3)	0.671 3 (4)	4.8 (2)
H2	0.292 (3)	0.267 (2)	0.337 (3)	1.9 (9)*	C4C	−0.285 3 (4)	0.113 2 (3)	0.150 2 (5)	4.2 (1)
P1	−0.047 19 (8)	0.294 07 (6)	0.333 31 (8)	2.08 (2)	C4D	0.511 4 (5)	0.233 7 (4)	0.787 8 (4)	6.0 (2)
P2	0.262 73 (8)	0.127 37 (6)	0.484 69 (8)	2.09 (2)	C4E	−0.029 8 (4)	0.092 3 (3)	0.493 6 (6)	7.3 (2)
P3	0.169 78 (8)	0.248 32 (6)	0.045 68 (8)	1.90 (2)	C4F	0.351 0 (4)	−0.105 3 (3)	0.408 4 (4)	4.3 (2)
P4	0.237 55 (8)	0.142 43 (6)	0.147 49 (8)	1.81 (2)	C4G	0.310 0 (4)	0.371 5 (3)	−0.096 5 (4)	4.1 (1)
P5	0.241 85 (7)	0.391 18 (6)	0.286 23 (8)	1.85 (2)	C4H	−0.155 8 (4)	0.247 4 (3)	−0.161 2 (4)	4.0 (1)
P6	0.390 66 (7)	0.310 00 (6)	0.259 26 (7)	1.77 (2)	C4I	0.522 7 (3)	0.027 0 (3)	0.207 2 (4)	3.4 (1)
C34	0.194 7 (3)	0.152 5 (2)	0.016 3 (3)	2.6 (1)	C4J	0.032 4 (4)	−0.021 1 (3)	0.159 7 (4)	4.0 (1)
C56	0.358 2 (3)	0.404 2 (2)	0.276 7 (3)	2.14 (9)	C4K	0.037 7 (4)	0.547 6 (3)	0.122 8 (4)	4.1 (1)
C1A	−0.100 4 (3)	0.376 1 (2)	0.301 0 (3)	2.12 (9)	C4L	0.323 3 (4)	0.497 3 (3)	0.628 3 (4)	4.6 (1)
C1B	−0.023 0 (3)	0.308 9 (2)	0.467 7 (3)	2.4 (1)	C4M	0.647 4 (3)	0.307 4 (3)	0.565 4 (3)	3.3 (1)
C1C	−0.143 3 (3)	0.223 1 (2)	0.262 5 (3)	2.6 (1)	C4N	0.559 7 (4)	0.272 3 (4)	0.054 1 (4)	4.5 (1)
C1D	0.375 2 (3)	0.169 1 (3)	0.608 5 (3)	2.7 (1)	C5A	−0.087 5 (4)	0.504 7 (3)	0.340 5 (4)	3.7 (1)
C1E	0.148 8 (3)	0.119 6 (2)	0.496 5 (3)	2.8 (1)	C5B	0.082 7 (5)	0.300 0 (3)	0.635 6 (4)	4.2 (1)
C1F	0.297 0 (3)	0.035 1 (2)	0.455 1 (3)	2.3 (1)	C5C	−0.268 6 (4)	0.146 3 (3)	0.250 4 (4)	4.2 (1)
C1G	0.223 5 (3)	0.293 4 (2)	−0.015 4 (3)	2.2 (1)	C5D	0.470 8 (5)	0.269 1 (4)	0.715 0 (4)	7.8 (2)
C1H	0.040 1 (3)	0.249 9 (2)	−0.033 2 (3)	2.3 (1)	C5E	0.050 5 (4)	0.111 2 (3)	0.586 5 (5)	6.1 (1)
C1I	0.350 4 (3)	0.096 6 (2)	0.171 3 (3)	2.14 (9)	C5F	0.281 6 (4)	−0.090 2 (3)	0.448 2 (4)	4.2 (1)
C1J	0.154 6 (3)	0.075 1 (2)	0.145 6 (3)	2.3 (1)	C5G	0.261 8 (4)	0.406 8 (3)	−0.037 3 (3)	3.5 (1)
C1K	0.161 8 (3)	0.453 8 (2)	0.221 3 (3)	2.2 (1)	C5H	−0.125 5 (4)	0.274 3 (3)	−0.059 2 (4)	4.3 (1)
C1L	0.266 6 (3)	0.433 4 (2)	0.420 4 (3)	2.09 (9)	C5I	0.449 7 (4)	0.010 6 (3)	0.111 8 (4)	3.4 (1)
C1M	0.492 9 (3)	0.307 4 (2)	0.379 8 (3)	2.06 (9)	C5J	−0.004 6 (4)	0.038 5 (3)	0.123 3 (4)	3.9 (1)
C1N	0.451 2 (3)	0.295 7 (3)	0.171 7 (3)	2.2 (1)	C5K	0.000 5 (4)	0.492 3 (3)	0.140 4 (4)	4.1 (1)
C2A	−0.180 9 (3)	0.376 0 (3)	0.211 8 (4)	3.0 (1)	C5L	0.332 6 (4)	0.535 7 (3)	0.565 1 (4)	4.3 (1)
C2B	−0.092 1 (3)	0.338 8 (3)	0.505 1 (4)	3.4 (1)	C5M	0.651 3 (4)	0.270 5 (3)	0.474 1 (4)	3.3 (1)
C2C	−0.161 2 (4)	0.190 4 (3)	0.162 2 (4)	3.6 (1)	C5N	0.515 4 (4)	0.215 2 (3)	0.062 2 (4)	3.8 (1)
C2D	0.397 3 (4)	0.132 8 (3)	0.684 0 (3)	3.5 (1)	C6A	−0.052 9 (3)	0.441 5 (3)	0.364 8 (3)	2.8 (1)
C2E	0.067 0 (4)	0.101 5 (3)	0.405 7 (4)	4.0 (1)	C6B	0.063 5 (4)	0.290 2 (3)	0.532 4 (3)	3.1 (1)
C2F	0.368 6 (4)	0.020 0 (3)	0.417 7 (4)	3.3 (1)	C6C	−0.198 3 (3)	0.200 8 (3)	0.306 8 (4)	3.4 (1)
C2G	0.269 2 (3)	0.258 9 (3)	−0.078 1 (3)	3.1 (1)	C6D	0.393 7 (5)	0.237 4 (3)	0.625 2 (4)	5.7 (2)
C2H	0.008 3 (4)	0.222 0 (3)	−0.138 7 (4)	3.6 (1)	C6E	0.141 9 (4)	0.124 8 (3)	0.588 5 (4)	3.8 (1)
C2I	0.425 5 (3)	0.113 5 (2)	0.267 8 (3)	2.3 (1)	C6F	0.254 7 (4)	−0.020 3 (3)	0.472 1 (4)	3.2 (1)
C2J	0.190 0 (4)	0.014 7 (3)	0.179 8 (3)	2.9 (1)	C6G	0.218 9 (4)	0.368 7 (3)	0.003 2 (3)	2.9 (1)
C2K	0.198 9 (4)	0.511 3 (3)	0.203 3 (3)	2.9 (1)	C6H	−0.028 0 (4)	0.275 5 (3)	0.005 2 (4)	3.3 (1)
C2L	0.254 6 (3)	0.396 7 (2)	0.483 8 (3)	2.7 (1)	C6I	0.362 6 (3)	0.044 7 (3)	0.092 2 (3)	2.9 (1)
C2M	0.489 4 (3)	0.344 0 (3)	0.471 8 (3)	2.9 (1)	C6J	0.055 7 (3)	0.086 5 (3)	0.117 1 (4)	3.3 (1)
C2N	0.493 0 (3)	0.354 3 (3)	0.160 4 (3)	2.9 (1)	C6K	0.063 0 (3)	0.445 1 (3)	0.190 9 (3)	3.1 (1)
C3A	−0.213 2 (4)	0.439 7 (3)	0.186 9 (4)	3.6 (1)	C6L	0.304 5 (4)	0.504 2 (3)	0.462 3 (4)	3.5 (1)
C3B	−0.073 1 (4)	0.347 6 (3)	0.605 9 (4)	4.4 (1)	C6M	0.574 7 (3)	0.270 1 (2)	0.381 3 (3)	2.7 (1)
C3C	−0.232 6 (4)	0.136 4 (3)	0.105 5 (4)	4.1 (1)	C6N	0.461 6 (3)	0.227 0 (3)	0.121 6 (3)	2.8 (1)
C3D	0.473 8 (5)	0.164 7 (4)	0.773 6 (4)	4.8 (2)	N1	0.243 6 (3)	0.046 1 (3)	0.793 0 (3)	3.5 (1)
C3E	−0.021 2 (4)	0.087 0 (3)	0.405 6 (6)	6.2 (2)	O1	0.168 5 (3)	0.048 9 (5)	0.804 8 (4)	11.6 (2)
C3F	0.394 6 (4)	−0.051 0 (3)	0.393 6 (4)	4.4 (1)	O2	0.316 7 (3)	0.076 8 (2)	0.863 7 (3)	4.7 (1)
C3G	0.312 3 (4)	0.298 2 (3)	−0.117 8 (4)	3.8 (1)	O3	0.245 9 (3)	0.010 3 (2)	0.710 6 (3)	3.9 (1)
C3H	−0.090 0 (4)	0.221 0 (3)	−0.201 7 (4)	4.3 (1)	N2	−0.418 (2)	0.440 (1)	−0.125 (2)	15.8 (8)*
C3I	0.511 4 (3)	0.078 6 (3)	0.287 2 (4)	3.1 (1)	O4	−0.411 5 (4)	0.449 9 (3)	−0.193 0 (4)	8.4 (2)
C3J	0.128 4 (4)	−0.033 2 (3)	0.186 4 (4)	3.8 (1)	O5	−0.359 5 (6)	0.403 4 (4)	−0.066 5 (7)	15.0 (3)
C3K	0.136 7 (4)	0.558 3 (3)	0.154 4 (4)	3.6 (1)	O6	−0.481 (2)	0.473 (2)	−0.105 (2)	26 (1)*
C3L	0.283 0 (4)	0.427 7 (3)	0.587 1 (3)	3.8 (1)					

[a] Starred atoms were refined isotropically. Anisotropically refined atoms are given in the form of the isotropic equivalent thermal parameter defined as $(4/3)[A^2B(1,1) + B^2B(2,2) + C^2B(3,3) + AB(\cos\gamma)B(1,2) + AC(\cos\beta)B(1,3) + BC(\cos\alpha)B(2,3)]$.

(2.370 (1) and 2.361 (1) Å) relative to those of the mutually trans phosphorus atoms (2.379 (1) and 2.335 (1) Å). This is in agreement with observations of others which clearly show that bridging hydrides do not exhibit a large trans influence.[25] If the hydrides in **1** were bonded to Ru in a terminal fashion, the Ru–P bonds trans to the hydrides are expected to be significantly longer. This is clearly evident in *cis*-$(H)_2Ru(dppe)_2$ where the Ru–P distances trans to the hydrides average 2.312 (3) Å compared with 2.283 (3) Å for those which are mutually trans.[26] The distances and angles within the ligands and nitrate counterions in **1** are normal (see supplementary material).[19]

It is important to note that while the μ-H ligands in **1** lie *transoid* to Ru–P vectors, they are not so disposed relative to the Au–P vectors. This is contrary to observations with the only other X-ray characterized M–μ-H–Au–P compounds, $(CO)_5Cr(\mu\text{-}H)AuPPh_3$ and $[(H)_2(PPh_3)_3Ir(\mu\text{-}H)AuPPh_3]BF_4$.[3,4] With reference to diagram I, the values of α and β are, respectively, for the CrAu and IrAu compounds and for **1** 155.4 (1), 170 (4)°; 155.3 (1)°, not available;[27] and 172.45 (3), 151 (1)°. In **1** the

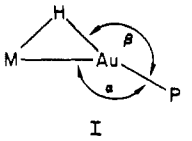

I

transition metal exerts the major stereoelectronic effect on Au, causing trans Ph_3P–Au–Ru stereochemistry, while in the Cr and Ir compounds the μ-H ligand dominates, resulting in trans Ph_3P–Au–μ-H stereochemistry. It is likely that the energy dif-

(25) Immirzi, A.; Porzio, W.; Bachechi, F.; Zambonelli, L.; Venanzi, L. M. *Gazz. Chim. It.* **1983**, *113*, 537.
(26) Pertici, P.; Vitulli, G.; Porzio, W.; Zocchi, M. *Inorg. Chim. Acta* **1979**, *37*, L521.
(27) The hydrogen position was not located in the X-ray analysis (ref 4).

Table III. Table of Positional Parameters and their Estimated Standard Deviations for **2**[a]

atom	X	Y	Z	B, Å²	atom	X	Y	Z	B, Å²
Au	0.273 80 (4)	0.048 62 (2)	0.266 00 (2)	2.396 (8)	C6E	0.271 (1)	0.181 7 (6)	0.147 7 (5)	4.0 (3)*
Ir	0.210 29 (4)	−0.035 10 (2)	0.195 33 (2)	1.860 (6)	C1F	0.064 (1)	0.094 3 (6)	0.142 5 (5)	2.9(3)*
P1	0.289 7 (3)	0.120 5 (1)	0.326 9 (1)	2.30 (6)	C2F	0.002 (1)	0.100 3 (6)	0.185 4 (5)	3.6 (3)*
P2	0.198 7 (3)	0.053 5 (1)	0.142 0 (1)	2.17 (6)	C3F	−0.100 (1)	0.133 7 (7)	0.187 8 (6)	4.4 (3)*
P3	0.206 6 (3)	−0.114 8 (1)	0.256 7 (1)	2.17 (6)	C4F	−0.139 (2)	0.158 9 (8)	0.144 4 (6)	5.6 (4)*
N	0.300 6 (9)	−0.090 4 (4)	0.144 5 (3)	2.4 (2)*	C5F	−0.079 (2)	0.156 9 (8)	0.101 8 (6)	5.1 (4)*
N′	0.083 9 (8)	−0.081 9 (4)	0.154 4 (3)	2.2 (2)*	C6F	0.022 (1)	0.123 4 (7)	0.100 2 (6)	4.4 (3)*
C2	0.243 (1)	−0.129 3 (5)	0.114 3 (4)	2.2 (2)*	C1G	0.219 (1)	−0.195 3 (5)	0.231 2 (4)	2.4 (2)*
C3	0.287 (1)	−0.168 9 (6)	0.079 2 (5)	3.6 (3)*	C2G	0.125 (1)	−0.221 3 (6)	0.207 3 (5)	3.5 (3)*
C4	0.406 (1)	−0.168 4 (7)	0.075 3 (6)	4.1 (3)*	C3G	0.127 (1)	−0.280 7 (7)	0.184 8 (5)	3.7 (3)*
C5	0.473 (1)	−0.130 1 (7)	0.104 9 (5)	3.7 (3)*	C4G	0.225 (1)	−0.315 3 (7)	0.186 9 (6)	4.9 (3)*
C6	0.418 (1)	−0.091 5 (6)	0.140 2 (5)	3.3 (3)*	C5G	0.318 (1)	−0.291 9 (7)	0.210 3 (5)	4.3 (3)*
C2′	0.120 (1)	−0.122 4 (6)	0.118 8 (4)	2.4 (2)*	C6G	0.316 (1)	−0.231 9 (6)	0.231 7 (5)	3.3 (3)*
C3′	0.042 (1)	−0.157 3 (8)	0.090 9 (6)	4.4 (3)*	C1H	0.080 (1)	−0.120 3 (6)	0.294 1 (4)	2.6 (2)*
C4′	−0.070 (1)	−0.149 1 (8)	0.099 7 (6)	4.5 (3)*	C2H	0.065 (1)	−0.175 8 (7)	0.324 0 (5)	3.5 (3)*
C5′	−0.109 (1)	−0.103 4 (6)	0.134 1 (5)	3.5 (3)*	C3H	−0.026 (1)	−0.179 8 (8)	0.355 7 (6)	4.7 (4)*
C6′	−0.027 (1)	−0.071 9 (6)	0.160 6 (5)	3.1 (3)*	C4H	−0.103 (1)	−0.131 2 (7)	0.356 7 (5)	4.1 (3)*
C1A	0.419 (1)	0.113 3 (6)	0.363 2 (4)	2.6 (2)*	C5H	−0.098 (1)	−0.077 9 (7)	0.327 0 (5)	4.0 (3)*
C2A	0.432 (1)	0.147 8 (6)	0.406 6 (5)	2.8 (2)*	C6H	−0.004 (1)	−0.072 7 (6)	0.296 1 (4)	2.9 (3)*
C3A	0.534 (1)	0.141 9 (7)	0.431 9 (5)	3.4 (3)*	C1I	0.319 (1)	−0.107 4 (6)	0.302 9 (5)	2.9 (2)*
C4A	0.618 (1)	0.100 0 (8)	0.414 8 (6)	4.8 (4)*	C2I	0.432 (1)	−0.101 2 (6)	0.288 0 (5)	3.0 (3)*
C5A	0.602 (1)	0.065 8 (7)	0.372 8 (6)	4.4 (3)*	C3I	0.518 (1)	−0.095 5 (7)	0.320 9 (5)	3.8 (3)*
C6A	0.504 (1)	0.072 7 (6)	0.346 6 (5)	3.3 (3)*	C4I	0.495 (1)	−0.094 6 (7)	0.369 7 (6)	4.3 (3)*
C1B	0.288 (1)	0.202 1 (5)	0.303 7 (4)	2.4 (2)*	C5I	0.387 (1)	−0.098 5 (8)	0.386 1 (6)	5.0 (4)*
C2B	0.191 (1)	0.219 3 (6)	0.277 2 (5)	3.6 (3)*	C6I	0.300 (1)	−0.105 9 (6)	0.353 9 (5)	3.5 (3)*
C3B	0.179 (1)	0.280 6 (7)	0.257 8 (5)	3.9 (3)*	B1	0.198 (1)	0.704 6 (7)	0.978 4 (5)	2.9 (3)*
C4B	0.260 (1)	0.325 3 (6)	0.267 0 (5)	3.5 (3)*	B2	0.321 (2)	0.508 5 (9)	0.283 5 (7)	5.5 (5)*
C5B	0.355 (1)	0.309 0 (7)	0.293 8 (5)	4.0 (3)*	F1	0.1201 (7)	0.739 1 (4)	1.001 4 (3)	4.7 (2)
C6B	0.365 (1)	0.247 1 (6)	0.312 2 (5)	3.2 (3)*	F2	0.1960 (8)	0.640 4 (4)	0.989 3 (3)	5.6 (2)
C1C	0.171 (1)	0.113 9 (5)	0.368 1 (4)	2.2 (2)*	F3	0.3081 (6)	0.729 6 (4)	0.989 4 (2)	3.8 (2)
C2C	0.140 (1)	0.166 6 (6)	0.398 7 (5)	2.9 (2)*	F4	0.1860 (6)	0.710 5 (4)	0.925 9 (2)	3.8 (2)
C3C	0.047 (1)	0.158 5 (7)	0.429 0 (5)	3.4 (3)*	F5	0.227 (1)	0.489 2 (5)	0.263 6 (6)	12.2 (4)
C4C	−0.015 (1)	0.105 4 (7)	0.428 6 (5)	3.6 (3)*	F6	0.345 (1)	0.567 2 (5)	0.267 1 (5)	11.0 (4)
C5C	0.014 (1)	0.052 4 (8)	0.399 3 (5)	4.4 (3)*	F7	0.302 (1)	0.519 9 (8)	0.334 7 (5)	14.9 (6)
C6C	0.109 (1)	0.058 2 (7)	0.369 3 (5)	3.6 (3)*	F8	0.408 (1)	0.471 6 (6)	0.281 5 (5)	10.3 (3)
C1D	0.214 (1)	0.027 8 (6)	0.078 2 (4)	3.0 (2)*	Cl1	0.1664 (8)	0.528 6 (4)	0.494 0 (3)	12.4 (2)*
C2D	0.319 (1)	0.028 9 (7)	0.056 0 (5)	4.1 (3)*	Cl2	0.379 (1)	0.557 4 (7)	0.463 7 (5)	23.2 (5)*
C3D	0.333 (2)	0.002 0 (8)	0.011 2 (6)	5.5 (4)*	C12	0.272 (2)	0.509 (1)	0.446 5 (8)	8.9 (6)*
C4D	0.241 (1)	−0.022 5 (7)	−0.017 1 (6)	5.4 (4)*	O	0.116 (1)	0.820 6 (7)	0.470 3 (6)	7.5 (4)*
C5D	0.138 (1)	−0.023 6 (7)	0.005 1 (5)	4.2 (3)*	CS1	0.015 (5)	0.781 (3)	0.501 (3)	22 (3)*
C6D	0.125 (1)	0.001 1 (6)	0.053 3 (5)	3.2 (3)*	CS2	0.001 (3)	0.730 (2)	0.531 (1)	20 (1)*
C1E	0.303 (1)	0.117 5 (5)	0.152 7 (4)	2.6 (2)*	CS3	0.216 (3)	0.796 (2)	0.501 (1)	21 (1)*
C2E	0.412 (1)	0.102 9 (6)	0.160 5 (5)	3.0 (3)*	CS4	0.259 (2)	0.278 (1)	0.028 (1)	12.7 (9)*
C3E	0.489 (1)	0.152 0 (8)	0.167 8 (6)	4.6 (3)*					
C4E	0.457 (1)	0.215 5 (7)	0.164 5 (6)	4.5 (3)*					
C5E	0.349 (1)	0.229 6 (7)	0.155 7 (5)	4.2 (3)*					

[a] Starred atoms were refined isotropically. Anisotropically refined atoms are given in the form of the isotropic equivalent thermal parameter defined as $(4/3)[A^2B(1,1) + B^2B(2,2) + C^2B(3,3) + AB(\cos\gamma)B(1,2) + AC(\cos\beta)B(1,3) + BC(\cos\alpha)B(2,3)]$.

ference between these two M-μ-H-Au-P stereochemistries is small, and there is evidence that **1** exhibits the *trans*-Ph_3P-Au-μ-H bonding mode ($\beta \approx 180°$) in solution (vide infra).

The $^{31}P\{^1H\}$ NMR spectrum of **1** (25 °C, CH_2Cl_2) is consistent with its solid-state structure. A trace of the spectrum is shown in Figure 3 and consists of three multiplets of equal intensity due to the three pairs of equivalent phosphorus atoms. The multiplet at δ 41.2 (P_A in Figure 3) is due to the gold phosphines. This assignment was made by observing the dppm methylene proton resonances while selectively decoupling the three phosphine resonances P_A, P_B, and P_C. Decoupling P_A had no effect on the methylene resonances, while decoupling P_B and P_C showed large effects which are consistent with decoupling one of the phosphorus atoms of the dppm ligand. The spectra for this selective decoupling experiment are included as supplementary material.[19] Therefore, P_B and P_C are assigned as dppm phosphorus atoms, and P_A is the equivalent PPh_3 phosphorus atoms. The assignment of P_B and P_C is less certain; however, a case can be made for the assignment shown in Figure 3. This is based on the observation that the P_C resonance is a clean triplet of triplets, whereas P_B is more complex. The two P_C phosphorus atoms couple to magnetically equivalent pairs of phosphorus atoms P_B and P_A. A P_B phosphorus atom on the other hand couples to two magnetically equivalent P_C atoms, to two magnetically nonequivalent P_A atoms, and with the magnetically nonequivalent other P_B atom, causing the P_B pattern to

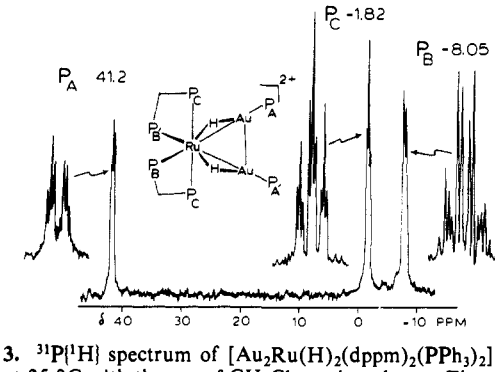

Figure 3. $^{31}P\{^1H\}$ spectrum of $[Au_2Ru(H)_2(dppm)_2(PPh_3)_2]^{2+}$, **1**, recorded at 25 °C with the use of CH_2Cl_2 as the solvent. The resonance due to internal standard trimethyl phosphate (δ 0) is omitted for clarity. The assignments of P_A, P_B, and P_C are discussed in the text.

be more complex. This assignment is confirmed in the selectively phosphorus-decoupled proton spectrum of the hydride resonance (Figure 4 and vide infra). The $^{31}P\{^1H\}$ spectrum has been successfully simulated assuming this $AA'BB'C_2$ assignment.[28]

(28) The PP coupling constants used in the simulation of the $^{31}P\{^1H\}$ NMR spectrum shown in Figure 3 are $J(P_C-P_A) = 8.5$, $J(P_C-P_B) = 33.0$, $J(P_A-P_B) = 36.3$, $J(P_A-P_{B'}) = 11.0$, $J(P_{A-A'}) = 18.0$, and $J(P_B-P_{B'}) = 18.0$.

Table IV. Selected Distances and Angles in the Coordination Core of $[Au_2Ru(H)_2(dppm)_2(PPh_3)_2](NO_3)_2$, **1**[a]

atom 1	atom 2	dist, Å	atom 1	atom 2	dist, Å	atom 1	atom 2	dist, Å
Au1	Au2	2.933 (0)	Ru	P5	2.379 (1)	P4	C34	1.841 (4)
Au1	Ru	2.786 (0)	Ru	P6	2.370 (1)	P4	C1I	1.817 (4)
Au1	H1	1.72 (4)	P1	C1A	1.818 (4)	P4	C1J	1.831 (4)
Au1	P1	2.278 (1)	P1	C1B	1.817 (4)	P5	C56	1.843 (4)
Au2	Ru	2.776 (0)	P1	C1C	1.820 (4)	P5	C1K	1.824 (4)
Au2	H2	1.82 (3)	P2	C1D	1.815 (4)	P5	C1L	1.833 (4)
Au2	P2	2.287 (1)	P2	C1E	1.806 (4)	P6	C56	1.833 (4)
Ru	H1	1.69 (4)	P2	C1F	1.818 (4)	P6	C1M	1.837 (4)
Ru	H2	1.53 (3)	P3	C34	1.839 (4)	P6	C1N	1.822 (4)
Ru	P3	2.361 (1)	P3	C1G	1.809 (4)			
Ru	P4	2.335 (1)	P3	C1H	1.829 (4)			

atom 1	atom 2	atom 3	angl, deg	atom 1	atom 2	atom 3	ang, deg	atom 1	atom 2	atom 3	ang, deg
Au2	Au1	Ru	58.00 (1)	H1	Ru	P4	82.0 (1)	Ru	P3	C34	95.2 (1)
Au2	Au1	H1	78.0 (1)	H1	Ru	P5	103.0 (1)	Ru	P3	C1G	122.8 (1)
Au2	Au1	P1	127.90 (3)	H1	Ru	P6	169.0 (1)	Ru	P3	C1H	123.5 (1)
Ru	Au1	H1	35.0 (1)	H2	Ru	P3	169.0 (1)	C34	P3	C1G	107.7 (2)
Ru	Au1	P1	170.69 (3)	H2	Ru	P4	102.0 (1)	C34	P3	C1H	103.8 (2)
H1	Au1	P1	147.0 (1)	H2	Ru	P5	83.0 (1)	C1G	P3	C1H	101.2 (2)
Au1	Au2	Ru	58.35 (1)	H2	Ru	P6	76.0 (1)	Ru	P4	C34	96.0 (1)
Au1	Au2	H2	74.0 (1)	P3	Ru	P4	71.67 (3)	Ru	P4	C1I	122.4 (1)
Au1	Au2	P2	121.14 (3)	P3	Ru	P5	102.39 (3)	Ru	P4	C1J	120.7 (1)
Ru	Au2	H2	31.0 (1)	P3	Ru	P6	96.62 (3)	C34	P4	C1I	106.3 (2)
Ru	Au2	P2	174.20 (3)	P4	Ru	P5	171.00 (3)	C34	P4	C1J	106.9 (2)
H2	Au2	P2	155.0 (1)	P4	Ru	P6	102.35 (3)	C1I	P4	C1J	102.7 (2)
Au1	Ru	Au2	63.65 (1)	P5	Ru	P6	71.18 (3)	Ru	P5	C56	94.1 (1)
Au1	Ru	H1	36.0 (1)	Au1	H1	Ru	109.0 (2)	Ru	P5	C1K	126.6 (1)
Au1	Ru	H2	82.0 (1)	Au2	H2	Ru	112.0 (2)	Ru	P5	C1L	121.1 (1)
Au1	Ru	P3	108.22 (3)	Au1	P1	C1A	109.1 (1)	C56	P5	C1K	104.9 (2)
Au1	Ru	P4	104.62 (2)	Au1	P1	C1B	119.0 (1)	C56	P5	C1L	104.0 (2)
Au1	Ru	P5	83.53 (2)	Au1	P1	C1C	110.1 (1)	C1K	P5	C1L	102.2 (2)
Au1	Ru	P6	147.84 (2)	C1A	P1	C1B	104.4 (2)	Ru	P6	C56	94.6 (1)
Au2	Ru	H1	83.0 (1)	C1A	P1	C1C	106.2 (2)	Ru	P6	C1M	119.8 (1)
Au2	Ru	H2	37.0 (1)	C1B	P1	C1C	107.1 (2)	Ru	P6	C1N	127.1 (1)
Au2	Ru	P3	142.92 (3)	Au2	P2	C1D	108.1 (1)	C56	P6	C1M	104.8 (2)
Au2	Ru	P4	75.73 (2)	Au2	P2	C1E	112.7 (1)	C56	P6	C1N	106.0 (2)
Au2	Ru	P5	111.86 (2)	Au2	P2	C1F	116.8 (1)	C1M	P6	C1N	101.5 (2)
Au2	Ru	P6	107.29 (2)	C1D	P2	C1E	109.9 (2)	P3	C34	P4	96.7 (2)
H1	Ru	H2	113.0 (2)	C1D	P2	C1F	104.4 (2)	P5	C56	P6	97.5 (2)
H1	Ru	P3	75.0 (1)	C1E	P2	C1F	104.4 (2)				

[a] Numbers in parentheses are estimated standard deviations to the least significant digits.

The ^1H NMR spectrum of **1** (25 °C, CD_2Cl_2) recorded in the hydride region with selective phosphorus decoupling is shown in Figure 4. The resonance is centered at δ −4.62. The selective P decoupling supports the assignment of P_B and P_C shown in Figure 3. Note that P_B decoupling gives a doublet of triplets, while P_C decoupling gives a doublet of doublets. The two P_C atoms are magnetically equivalent with respect to a μ-H, so a triplet pattern [$^2J(H-P_C)$ = 8.1 Hz] results when P_B is decoupled. The two P_B atoms are magnetically nonequivalent with respect to a μ-H and only the P_B atom which is approximately trans to the μ-H couples, giving a doublet pattern [$^2J(H-P_B)$ = 6.2 and $^2J(H-P_{B'}) \approx 0$ Hz] when P_C is decoupled. Both of these patterns are doubled due to coupling between μ-H and P_A [$^2J(H-P_A)$ = 74.8, $^3J(H-P_{A'}) \approx 0$ Hz]. The P_A-decoupled spectrum is consistent with the above analysis. The nondecoupled hydride pattern has been successfully simulated by using the above coupling constants.

An important result of the NMR analysis is that the $^2J(\mu$-H-$P_A)$ coupling constant in the μ-*H*Au*P*Ph$_3$ unit is 74.8 Hz. This is comparable to the values of 79.4 Hz in $[(H)_2(PPh_3)_3Ir(\mu$-*H*)-Au*P*Ph$_3$]BF_4[4] and 105 Hz in $(CO)_5Cr(\mu$-*H*)Au*P*Ph$_3$[3] and is as expected for a *transoid* Ph_3P–Au–H arrangement.[3] However, in the solid state, **1** does not have the trans Ph_3P–Au–H arrangement (vide supra and Figure 1). Although it is not known what effect a decrease in β (see I) from ca. 170° to ca. 155° has on $J(\mu$-H-P), it is expected to be large (vide infra). It is most likely that in solution **1** has the trans Ph_3P–Au–H stereochemistry. Referring to the solid-state structure shown in Figure 1, this represents a downward displacement of P1 an equal upward displacement of P2. A careful examination of the solid-state geometry of **1** shows

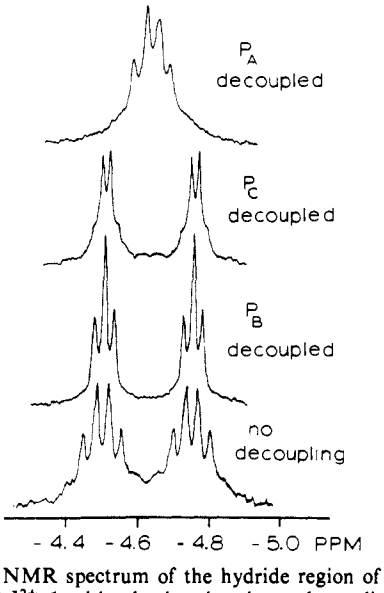

Figure 4. ^1H NMR spectrum of the hydride region of $[Au_2Ru(H)_2(dppm)_2(PPh_3)_2]^{2+}$, **1**, with selective phosphorus decoupling, recorded at 25 °C with the use of CD_2Cl_2 as the solvent. See Figure 3 for the assignment of the decoupled phosphorus resonances.

that these phosphorus atoms are already displaced a small amount in these directions. Displacements from the $RuAu_2$ plane are H1 (+0.87 Å), P1 (−0.28 Å), H2 (−0.86 Å), and P2 (+0.23 Å). It

Table V. Selected Distances and Angles in the Coordination Core of $[AuIr(H)_2(bipy)(PPh_3)_3](BF_4)_2$, **2**[a]

atom 1	atom 2	dist, Å	atom 1	atom 2	dist, Å	atom 1	atom 2	dist, Å
Au	Ir	2.699 (0)	N	C2	1.339 (12)	C4	C5	1.38 (2)
Au	P1	2.239 (2)	N	C6	1.407 (14)	C5	C6	1.41 (2)
Ir	P2	2.349 (2)	N′	C2′	1.353 (12)	C2′	C3′	1.40 (2)
Ir	P3	2.352 (2)	N′	C6′	1.344 (14)	C3′	C4′	1.36 (2)
Ir	N	2.094 (8)	C2	C3	1.360 (14)	C4′	C5′	1.41 (2)
Ir	N′	2.109 (8)	C2	C2′	1.475 (14)	C5′	C6′	1.38 (2)
N	N′	2.601 (13)	C3	C4	1.43 (2)			

atom 1	atom 2	atom 3	ang, deg	atom 1	atom 2	atom 3	ang, deg	atom 1	atom 2	atom 3	ang, deg
Ir	Au	P1	168.58 (9)	N	Ir	N′	76.4 (4)	C4	C5	C6	118.0 (1)
Au	Ir	P2	86.66 (6)	Ir	N	N′	52.0 (3)	N	C6	C5	112.0 (1)
Au	Ir	P3	87.88 (6)	Ir	N′	N	51.5 (3)	N′	C2′	C2	116.0 (9)
Au	Ir	N	132.7 (3)	C2	N	C6	116.6 (9)	N′	C2′	C3′	120.0 (1)
Au	Ir	N′	150.7 (2)	C2′	N′	C6′	120.1 (9)	C2	C2′	C3′	124.0 (1)
P2	Ir	P3	171.72 (9)	N	C2	C3	127.0 (1)	C2′	C3′	C4′	119.0 (1)
P2	Ir	N	93.5 (2)	N	C2	C2′	113.3 (9)	C3′	C4′	C5′	121.0 (1)
P2	Ir	N′	90.0 (2)	C3	C2	C2′	120.0 (1)	C4′	C5′	C6′	116.0 (1)
P3	Ir	N	94.8 (2)	C2	C3	C4	115.0 (1)	N′	C6′	C5′	124.0 (1)
P3	Ir	N′	91.7 (2)	C3	C4	C5	122.0 (1)				

[a] Numbers in parentheses are estimated standard deviations to the least significant digits.

is likely that these displacements of P1 and P2 are accompanied by similar displacements of the dppm phosphorus atoms. This would be necessary to relieve steric repulsions between phenyl rings. The value of $^2J(H-P_B)$ is only 6.2 Hz. A much larger value is expected for a trans μ-H-M-P coupling,[4,29] and therefore, dppm phosphorus displacements such that P3 and P6 become approximately trans to Au atoms are reasonable and consistent with the NMR data.

The infrared spectrum of **1** was measured in the solution (CH_2Cl_2) and solid (KBr disk) phases, and no peaks in the terminal hydride stretching region (1700–2300 cm^{-1}) were observed. Unfortunately, the bridging region (800–1400 cm^{-1}) is complicated by many intense absorptions of the compound.

$[AuIr(H)_2(bipy)(PPh_3)_3](BF_4)_2$, 2. Previous work on the reaction between $[Ir(H)_2(PPh_3)_2(acetone)_2]BF_4$ and $AuPPh_3NO_3$ in acetone solution at −35 °C showed that the adduct $[(NO_3)(PPh_3)_2Ir(H)_2AuPPh_3]BF_4$, **3**, formed.[7,11] It was suggested that **3** contained bridging hydrides; however, due to its instability an X-ray analysis could not be carried out. The coupling constant between the equivalent hydrides and the gold phosphine phosphorus was 30 Hz which is larger than expected for a nonbridging *H*–Ir–Au–*P* arrangement (0–13 Hz)[4,7] but small compared to known bridging $Ir(\mu H)AuPPh_3$ coupling constants (vide supra, 75–100 Hz).[3,4] It was thought that **3** contained one bridging and one terminal hydride which exchanged rapidly on the NMR time scale. This would result in a H–P coupling constant which is an average between the terminal (0–13 Hz) and bridging values (75–100 Hz) and therefore in the range of the 30 Hz observed. Alternatively, rapid exchange between *trans*-Ir-Au–PPh_3 and *trans*- and *cis*-H–Au–PPh_3 arrangements for a dihydrido-bridged formulation would lead to an H–P coupling constant which is averaged over these arrangements and therefore also expected to be in the 30-Hz range (see discussion on **1**). The synthesis of the bipyridyl analogue $[(bipy)(PPh_3)_2Ir(H)_2AuPPh_3](BF_4)_2$, **2**, was carried out in order to see if the questions about hydride bonding and stereochemistry could be answered and to further probe the mechanism of formation of Au–Ir clusters in general.[6-8]

Compound **2** was synthesized in high yield from the reaction of $[Ir(H)_2(PPh_3)_2(bipy)]BF_4$ with $AuPPh_3NO_3$ in acetone solution. **2** was found to be stable and resisted further reaction with $AuPPh_3NO_3$, contrary to **3** which readily formed $[Au_2Ir(H)(PPh_3)_4(NO_3)_3]BF_4$ and eventually $[Au_3Ir(PPh_3)_5(NO_3)]BF_4$.[7,8] Crystals of **2** were also suitable for an X-ray analysis which was carried out at −50 °C. The structure consisted of well-separated dications, BF_4^- anions, and CH_2Cl_2 and Et_2O solvate molecules. The structure of the coordination core of **2** is shown in Figure 2, and distances and angles are given in Table V. The hydride ligands were not located, but a case will be made for a dibridging formulation (vide infra). The structure consists of a planar $(N)_2IrAuP$ arrangement with the linear P2–Ir–P3 (171.72 (9)°) grouping perpendicular to this plane. The primed and unprimed halves of the bipy ligand are planar within experimental error, and the dihedral angle between these planes is only 3°. The IR atom is displaced 0.09 Å from the least-squares plane of the bipy ligand. Distances and angles within the bipy ligand are normal.[30,31] The Ir–N distances (average 2.102 (8) Å) are comparable to those observed in other bipy complexes of Ir(III) [average 2.04 (1) Å in $[Ir(bipy)_3](ClO_4)_3$,[30] 2.053 (5) and 2.135 (5) Å for Ir–N trans to N- and C-bonded bipy, respectively, in $[Ir(bipy\text{-}C,N)(bipy\text{-}N,N')_2](ClO_4)_3$[31]]. The Ir–P distances (average 2.351 (2) Å) are comparable to values found for trans PPh_3 ligands in other IrAu clusters.[6-8]

The Au–Ir distance in **2** (2.699 (0) Å) is long compared with the non-hydrido compound $[(dppe)_2IrAuPPh_3](BF_4)_2$[32] (2.625 (1) Å), short compared with the hydrido-bridged compound $[(PPh_3)_3(H)_2Ir(\mu\text{-}H)AuPPh_3]BF_4$[4] (2.765 (1) Å), and comparable to averaged values observed in a variety of AuIr clusters [2.685 (1) Å in $[Au_2IrH(PPh_3)_4(NO_3)]BF_4$,[7] 2.641 (1) Å in $[Au_3Ir(PPh_3)_5(NO_3)]BF_4$,[8] and 2.690 (2) Å in $[Au_4Ir(H)_2(PPh_3)_6]BF_4$].[6] It is not possible to establish a reliable trend here concerning the mode of hydride bonding due to the small number of similar compounds whose structures are known. However, it does appear that the compounds with $M(\mu\text{-}H)Au$ bonding have the longest M–Au separations. For example, M–Au distances in **1** (average 2.781 (0) Å), $[(PPh_3)_3(H)_2Ir(\mu\text{-}H)AuPPh_3]BF_4$ (2.765 (1) Å),[2] and $(CO)_5Cr(\mu\text{-}H)AuPPH_3$ (2.770 (2) Å)[3] are among the longest in MAu_x phosphine clusters. In $[Au_3Rh(H)(CO)(PPh_3)_5]PF_6$, which is through to have one hydrido-bridged Au–Rh bond and two which do not have hydride bridges, the Au–Rh separations are 2.722 (3) and average 2.652 (3) Å, respectively.[5] A similar result has been observed in $[Au_4Ir(H)_2(PPh_3)_6]BF_4$ which has averaged Au–Ir separations of 2.724 (2) and 2.622 (2) Å, respectively, for μ-H and non-μ-H bonds.[6] In these latter two compounds, the hydrides have not been observed directly by X-ray diffraction, but their positions were deduced from a combination of NMR and structural analyses. Since the Au–Ir separation in

(29) Wang, H. H.; Pignolet, L. H. *Inorg. Chem.* **1980**, *19*, 1470.

(30) Hazell, A. C. *Abstracts*, 18th Danish Crystallography Meeting, Risø, Denmark; Wiley: New York, 1982; paper 24.

(31) Nord, G.; Hazell, A. C.; Hazell, R. G.; Farver, O. *Inorg. Chem.* **1983**, *22*, 3429.

(32) Casalnuovo, A. L.; Laska, T.; Nilsson, P. V.; Olofson, J.; Pignolet, L. H. *Inorg. Chem.* **1985**, *24*, 233.

2 is significantly longer than in $[(dppe)_2IrAuPPh_3](BF_4)_2$,[32] it is likely that bridging hydride ligands are present. It has been established in general that mono-hydrogen-bridged M-μ-HM bonds are longer than unbridged M–M bonds.[21]

The Au–P distance in **2** (2.239 (2) Å) is short compared with values observed in the known $Ir(AuPPh_3)_x$ clusters with $x > 1$ (range from ca. 2.25 to 2.31 Å[6-8]) and slightly long compared with the 2.219 (5) Å value observed in $[AuIr(dppe)_2(PPh_3)](BF_4)_2$.[32] In all of these compounds the Au–P vector is ca. trans to the Ir atom. The higher coordination numbers for Au in the $x > 1$ compounds probably account for their longer Au–P distances.

The Ir–Au–P angle in **2** (168.6 (1)°) is similar to values found in $[(dppe)_2IrAu(PPh_3)](BF_4)_2$[32] (168.7 (5)°) and in **1** (172.45 (3)°). This approximate trans M–Au–PPh_3 stereochemistry has been observed in all of the $M(AuPPh_3)_x$ clusters with $x > 1$ in the solid state[5-8] and seems to be characteristic of this class of compound. The effect of bridging hydrides on this sterochemistry has been discussed above, and unfortunately the trans Ir–Au–PPh_3 arrangement in **2** does not argue for or against a bridging hydride formulation.

The Au–Ir–N angles are significantly different [132.7 (3)° and 150.7 (2)°, respectively, for angles involving N and N']. A distortion of a similar magnitude has been observed in $[(dppe)_2IrAuPPh_3](BF_4)_2$ where the Ir–Au vector is tilted ca. 15° for the normal to the IrP_4 plane.[32] This distortion in **2** is probably due to packing forces but could also result from unsymmetrically positioned hydride ligands. For example, one bridging hydride and either one nonbridging (terminal or Ir) or one semibridging hydride is possible. In order to address these possibilities, a calculation has been carried out using atomic parameters from the X-ray analysis. If the hydride ligands are positioned exactly trans to the Ir–N vectors (H trans to N and H' trans to N') and the Ir–H distances are set at 1.7 Å, the following values result: Au–H, 1.99 Å; Au–H', 1.47 Å; Ir–H–Au, 94°; Ir–H'–Au, 116°. Both hydrides are asymmetrically bridging in this model, but if values are averaged for the primed and nonprimed hydrides, reasonable bridging values result: Ir–H, 1.70 Å; Au–H, 1.73 Å; Ir–H–Au, 105°. This is to say that if the geometry were idealized so that both N–Ir–Au angles were the same, a symmetric dihydride-bridged arrangement would result. From these arguments alone it is not possible to prove a dihydride-bridged arrangement; however, this arrangement is implicated by NMR and IR results. The NMR data implicate significant gold–hydride interaction (vide infra). Finally, the fact that the two Ir–N distances are the same within experimental error is consistent with a dihydride-bridged arrangement.

The $^{31}P\{^1H\}$ NMR spectrum of **2** (25 °C, CH_2Cl_2) is in agreement with its solid-state structure and consists of two singlet resonances (δ 46.5 and 2.98) with an intensity ratio of 1:2. These resonances are due to the gold and iridium phosphines, respectively. The ^1H NMR (25 °C, $CDCl_3$) spectrum consisted of a doublet of triplets centered at δ −13.3 with J = 31 and 11 Hz for the doublet and triplet splittings, respectively. Selective phosphorus decoupling confirmed that the 31-Hz doublet coupling was due to the gold-bound phosphorus atom. The ^{31}P and ^1H NMR data are very similar to that observed for the analogue with NO_3 replacing bipy, **3**,[7,11] [^{31}P NMR (−35 °C): δ 44.8 (s, int = 1), 5.14 (s, int = 2). ^1H NMR (−35 °C): δ −17.5 (d of t, J = 30 and 10 Hz)]. Therefore, compounds **2** and **3** must have the same $Ir(H)_2AuP$ stereochemistry. The magnitude of the $HAuPPh_3$ coupling constants in these two compounds and the arguments presented above favor a dihydride-bridged arrangement in solution with the gold phosphorus atom in rapid equilibrium between *trans*-Ir–Au–P and *trans*- and *cis*-μ-H–Au–P stereochemistries. Consistent with this formulation, **2** and **3** showed no IR absorptions in the terminal hydride stretching region (1700–2300 cm^{-1}) in solid or solution phase. In contrast both precursor compounds $[(acetone)_2Ir(H)_2(PPh_3)_2]BF_4$ and $[(bipy)Ir(H)_2(PPh_3)_2]BF_4$ showed distinct IR absorptions at 2228, 2240 cm^{-1} and 2215, 2240 cm^{-1}, respectively, in the solution phase. Although the absence of terminal hydride stretching absorptions is indirect evidence for the presence of bridging hydrides, the data presented in the next section show that terminal iridium hydrides in IrAu clusters are generally observable.

Other Iridium–Gold Hydrides. Two IrAu hydrides have been synthesized in which the hydrides are bonded in a terminal fashion to iridium. The reaction of $IrH(CO)(PPh_3)_3$ with 1 equiv of $AuPPh_3NO_3$ in toluene solvent followed by metathesis with KPF_6 gave the 1:1 adduct $[AuIrH(CO)(PPh_3)_4]PF_6$, **4**, in good yield. The proposed stereochemistry of **4** is shown in the drawing and has been deduced from ^{31}P and ^1H NMR and IR spectroscopies.

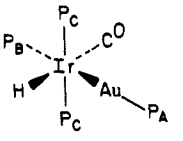

4

At temperatures above 25 °C the $^{31}P\{^1H\}$ NMR showed **4** to be nonrigid. The 85 °C spectrum (1,1,2-trichloroethane solvent) consisted of a quartet [δ 37.0 (J = 37 Hz, int = 1)] and a doublet [δ 5.7 (J = 37 Hz, int = 3)]. As the temperature was lowered to −40 °C (CH_2Cl_2 solvent), the quartet broadened and changed into a doublet [P_A δ 37.5 (J = 99 Hz, int = 1)] and the doublet broadened and changed into a new doublet [P_B δ 7.37 (J = 99 Hz, int = 1)] and a singlet [P_C δ 4.8 (int = 2)]. This is consistent with structure **4** and a dynamic process which interchanges the B and C phosphorus environments. The only observable coupling is between the gold-bound phosphorus P_A and trans P_B. All other PP coupling constants are less than ca. 7 Hz and therefore not resolved. The 37-Hz P_A–$P_{B,C}$ coupling constant in the −85 °C spectrum is therefore a 1:2 weighted average of $J(P_A–P_B)$ = 99 Hz and $J(P_A–P_C) \leq 6$ Hz. A value of $J(P_A–P_C)$ = 6 Hz gives the observed 37-Hz coupling constant. The ^1H NMR spectrum (acetone-d_6, 25 °C) recorded in the hydride region consisted of a quartet [(δ −8.9 (J_{PH} = 17 Hz)] due to coupling to the rapidly interchanging P_B and two P_C phosphorus atoms. The coupling between P_A and the hydride was too small to be observed and is indicative of a nonbridging hydride. The terminal hydride formulation was confirmed by the observation of ν_{IrH} 2060 cm^{-1} in the IR spectrum (KBr disk).

It is interesting that **4** is the only IrAu product observed when $AuPPh_3NO_3$ is reacted with $IrH(CO)(PPh_3)_3$. The same reaction with $RhH(CO)(PPh_3)_3$ gives the cluster $[Au_3RhH(CO)(PPh_3)_5]^+$ in good yield.[5] This reactivity difference may result from the greater tendency of $RhH(CO)(PPh_3)_3$ to dissociate PPh_3.

The reaction of $[Au_2IrH(NO_3)(PPh_3)_4]BF_4$[7] with 2 equiv of PPh_3 in an EtOH–Et_2O solvent mixture gave $[Au(PPh_3)_2]^+$ and $[AuIrH(PPh_3)_4]^+$, **5**, in quantitative yield. **5** is unstable in solution at 25 °C and was isolated in the solid state as a mixed BF_4–NO_3 salt. The reaction of **5** in acetone solution with CO lead to the formation of **4**. The proposed stereochemistry of **5** is shown in the drawing and has been deduced from ^{31}P and ^1H NMR and IR spectroscopies. The $^{31}P\{^1H\}$ NMR (0 °C, acetone) of **5**

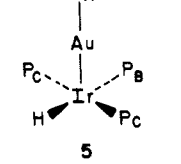

5

consisted of three resonances with relative intensities of 2:1:1 [P_C δ 28.1 (pseudo triplet), 19.5 (pseudo quartet), and −6.6 (pseudo quartet)]. In this spectrum P_A, P_B, and P_C are all coupled to each other with P–P coupling constants of approximately equal magnitude (8–10 Hz), and this gives rise to the observed splitting patterns. The P_A and P_B resonances have not been assigned. The ^1H NMR (0 °C, acetone-d_6) recorded in the hydride region consisted of a doublet of triplets of doublets pattern centered at δ −6.10. The coupling pattern and J values are consistent with the proposed structure of **5** [doublet, $^2J(H–P_B)$ = 99.5 Hz; triplet, $^2J(H–P_C)$ = 23.2 Hz; doublet, $^3J(H–P_A)$ = 4.1 Hz]. The terminal hydride formulation of **5** was confirmed by the observation of ν_{IrH}

2080 cm^{-1} in the IR spectrum (KBr disk).

Compounds **4** and **5** contrast with the other monotransition metal-gold hydrides (**1-3** and those listed in the Introduction[3-7]) in that they clearly do not have gold-hydride interactions. In all of the other compounds gold-hydride interactions have either been demonstrated[3,4] or are considered very likely.[5-7] The factors which influence the stability of gold-hydride interactions are not well understood, and it is clear that more studies of the type reported in this paper are needed.

Summary. Two new transition metal-gold hydrides $[Au_2Ru(H)_2(dppm)_2(PPh_3)_2](NO_3)_2$ (**1**) and $[AuIr(H)_2(bipy)(PPh_3)_3](BF_4)_2$ (**2**) have been synthesized. In **1** the hydride positions were located and refined by single-crystal X-ray crystallography and were found to be dibridging the Ru to Au bonds. In **2** the hydride positions were deduced from X-ray crystallography and NMR spectroscopy and are dibridging the IR to Au bond. ^{31}P and ^{1}H NMR results indicate significant gold-hydride interaction as determined by large spin-spin coupling between the hydride ligands and the gold phosphine phosphorus atoms. These results are important not only because gold-hydride interactions are rare but because they strongly imply that gold-hydride interactions are likely in a variety of gold-alloy hydride clusters. The trans M-Au-PPh_3 stererochemistry which has been found in **1** and **2** is also present in $[Au_5Re(H)_4(PPh_3)_7](PF_6)_2$,[5] $[Au_3RhH(CO)(PPh_3)_5]PF_6$,[5] $[Au_4Ir(H)_2(PPh_3)_6]BF_4$,[6] and $[Au_2IrH(PPh_3)_4(NO_3)]BF_4$.[7] In addition all of these compounds lack a terminal metal-hydride stretch in the IR spectrum although such an absorption was easily observed in $[AuIrH(CO)(PPh_3)_4]^+$ (**4**) and $[AuIrH(PPh_3)_4]^+$ (**5**). Compounds **4** and **5** have terminally bound iridium hydride ligands. The conclusions from this study are as follows: (i) a hydride ligand which bridges to gold does not require a trans μ-H-Au-PPh_3 stereochemistry as previously thought,[3-7] and (ii) gold-hydride interactions are probably much more prevalent in gold-alloy cluster hydrides than thought previously.[3-7]

Acknowledgment. This work has been supported by the National Science Foundation and by the University of Minnesota Graduate School. We thank the Johnson-Matthey Co. and Engelhard, Inc., for generous loans of iridium and ruthenium salts, respectively. Brian J. Johnson thanks Amoco for an industrial fellowship.

Registry No. 1, 102538-84-1; **2**, 102575-52-0; **4**, 102538-86-3; **5** (X = BF_4), 102538-88-5; **5** (X = NO_3), 102628-79-5; $AuPPh_3NO_3$, 14897-32-6; $Ru(H)_2(dppm)_2$, 89613-08-1; $[Ir(H)_2(PPh_3)_2(acetone)_2]BF_4$, 72414-17-6; $[Ir(H)_2(bpy)(PPh_3)_2]BF_4$, 102538-90-9; $IrH(CO)(PPh_3)_3$, 17250-25-8; $[Au_2IrH(NO_3)(PPh_3)_4]BF_4$, 93895-71-7; Ru, 7440-57-5; Au, 7440-57-5; Ir, 7439-88-5.

Supplementary Material Available: ORTEP drawings of **1** and **2** and the ^{1}H NMR spectrum of the dppm methylene resonances of **1** with selective ^{31}P decoupling (Figures S1-S3) and listings of general temperature factor expressions, calculated hydrogen atom positional parameters, distances and angles, least-squares planes, and observed and calculated structure factor amplitudes for **1** and **2** (Tables S1-S12) (96 pages). Ordering information is given on any current masthead page.

Kinetics and Mechanisms of Carbonyl Substitution Reactions of Bis(η^5-cyclopentadienyl) Dicarbonyl Compounds of the Titanium Triad Metals

G. Todd Palmer,[†] Fred Basolo,*[†] Larence B. Kool,[‡] and Marvin D. Rausch*[‡]

Contribution from the Department of Chemistry, Northwestern University, Evanston, Illinois 60201, and the Department of Chemistry, University of Massachusetts, Amherst, Massachusetts 01003. *Received November 15, 1985*

Abstract: Kinetic studies were performed for CO substitution reactions of $(\eta^5\text{-ring})_2M(CO)_2$, where $(\eta^5\text{-ring})$ = Cp, Cp*, or Ind[1] and M = Ti, Zr, or Hf. Nucleophiles used for these reactions include PMe_2Ph, $PMePh_2$, PPh_3, $P(OEt)_3$, $P(n\text{-}Bu)_3$, and CO. The reaction rates of the titanium compounds were first order in substrate and zero order in entering nucleophile at nucleophile concentrations which gave the limiting reaction rate. The results indicate a dissociative mechanism. Activation parameters for these reactions are also in agreement with a dissociative process. In contrast, reaction rates of the zirconium and hafnium compounds are first order in both substrate and entering nucleophile, indicating an associative mechanism. This mechanistic difference may be attributed to steric considerations caused by the smaller size of titanium. Equilibrium constants and rate constants indicate a strong preference of the Ti, Zr, and Hf metallocene compounds for CO over PR_3.

Studies on cyclopentadienyltitanium triad metal carbonyl compounds have increased,[2,3] since the first example, bis(η^5-cyclopentadienyl)titanium dicarbonyl, was reported by Murray[4] in 1959. The primary method of synthesis for these compounds is through reduction of the bis(η^5-cyclopentadienyl)metal dichloride in the presence of CO. Numerous reducing agents such as sodium,[5] electric current,[6] aluminum,[7] and magnesium[8] have been used.

Work on the titanium triad of metallocene has included substituting a carbonyl ligand by a phosphine or phosphite group. One of the reactions[9] for $Cp_2M(CO)(PR_3)$ formation is shown in eq 1, where M = Ti, Zr, or Hf and L = PR_3. Refluxing the

$$Cp_2M(CO)_2 + L \xrightarrow{\text{reflux}} Cp_2M(CO)(L) + CO \qquad (1)$$

reaction solutions is essential in order to remove generated CO from the solution. A method of synthesis for $Cp_2Ti(CO)(PR_3)$

[†] Northwestern University.
[‡] University of Massachusetts.

(1) Cp = η^5-cyclopentadienyl, Cp* = η^5-pentamethylcyclopentadienyl, and Ind = η^5-indenyl.

(2) Sikora, D. J.; Macomber, D. W.; Rausch, M. D. *Adv. Organomet. Chem.*, in press.
(3) Bottrill, M.; Gavens, P. D.; McMeeking, J. *Comprehensive Organometallic Chemistry*; Pergamon: Oxford, 1981; Vol. 3, pp 285-291.
(4) (a) Murray, J. G. *J. Am. Chem. Soc.* **1959**, *81*, 752-753. (b) Murray, J. G. *J. Am. Chem. Soc.* **1961**, *83*, 1287-1289.
(5) (a) Van Tamelan, E. E.; Cretney, W.; Klaentschi, N.; Miller, J. S. *J. Chem. Soc., Chem. Commun.* **1972**, 481-482. (b) Clauss, K.; Bestian, H. *Justus Liebigs Ann. Chem.* **1962**, *654*, 8-19.

0002-7863/86/1508-4417$01.50/0